ELSEVIER

Biochemical Pharmacology 62 (2001) 119–128

Biochemical Pharmacology

The effect of aliphatic, naphthenic, and aromatic hydrocarbons on production of reactive oxygen species and reactive nitrogen species in rat brain synaptosome fraction: the involvement of calcium, nitric oxide synthase, mitochondria, and phospholipase A

Oddvar Myhre[a,b,*], Frode Fonnum[a,b]

[a]*Norwegian Defence Research Establishment, Division for Protection and Material, P.O. Box 25, N-2027 Kjeller, Norway*
[b]*VISTA (The Norwegian Academy of Science and Letters/Statoil)*

Received 1 August 2000; accepted 16 January 2001

Abstract

This study investigated the effects of C7 and C9 aliphatic (*n*-heptane, *n*-nonane), naphthenic (methylcyclohexane, 1,2,4-trimethylcyclohexane (TMCH)) and aromatic (toluene, 1,2,4-trimethylbenzene (TMB)) hydrocarbons on the production of reactive oxygen species (ROS) and reactive nitrogen species (RNS) in rat brain synaptosome fraction. Methyl mercury (MeHg) was included as a positive control. Exposure of the synaptosomes to the hydrocarbons produced a concentration-dependent linear increase in the formation of the fluorescence of 2′,7′-dichlorofluorescein (DCF) as a measure of the production of ROS and RNS. Formation of RNS was demonstrated by preincubation of the synaptosome fraction with the neuronal nitric oxide synthase (nNOS) inhibitor Nω-nitro-L-arginine methyl ester (L-NAME), which reduced the MeHg and TMCH-stimulated fluorescence by 51% and 65%, respectively. The naphthenic hydrocarbon TMCH showed the strongest potential for ROS and RNS formation in rat brain synaptosomes, followed by TMB, toluene, *n*-nonane, *n*-heptane, and methylcyclohexane, respectively. TMCH was selected for mechanistic studies of the formation of ROS. Both MeHg and TMCH induced an increase in intracellular calcium concentration $[Ca^{2+}]_i$ as measured with Fura-2. Blockade of voltage-dependent Ca^{2+} channels with lanthanum prior to stimulation with MeHg and TMCH led to a reduction in the ROS/RNS formation of 72% and 70%, respectively. Furthermore, addition of cyclosporin A (CSA), a blocker of the mitochondrial permeability transition pore (MTP), lowered both the MeHg and TMCH-elevated DCF fluorescence by 72% and 59%. Preincubation of the synaptosome fraction with the protein tyrosine kinase inhibitor genistein lowered the MeHg and TMCH-stimulated fluorescence by 85% and 91%, respectively. Addition of the extracellular signal-regulated protein kinase (MEK)-1 and -2 inhibitor U0126 reduced the fluorescence stimulated by MeHg and TMCH by 62% and 63%. Furthermore, the protein kinase C inhibitor bisindolylmaleimide reduced the fluorescence stimulated by MeHg and TMCH by 52% and 56%. The compound 1-(6-[17beta-3-methoxyestra- 1,3,5(10)-trien- 17-yl]-aminohexyl)-1*H*-pyrrole-2,5-dione (U73122), which inhibits phospholipase C, was shown to decrease the ROS and RNS formation induced by MeHg and TMCH by 49% and 64%, respectively. The phospholipase A_2 (PLA_2) inhibitor 7,7-dimethyl eicosadienoic acid (DEDA) reduced fluorescence in response to MeHg and TMCH by 49% and 54%. Simultaneous addition of L-NAME, CSA, and DEDA to the synaptosome fraction totally abolished the DCF fluorescence. In conclusion, C7 and C9 aliphatic, naphthenic, and aromatic hydrocarbons stimulated formation of ROS and RNS in rat brain synaptosomes. The naphthenic hydrocarbon TMCH stimulated formation of ROS and RNS in the synaptosomes through Ca^{2+}-dependent activation of PLA_2 and nNOS, and through increased transition permeability of the MTP. Exposure of humans to the naphthenic hydrocarbon TMCH may stimulate formation of free radicals in the brain, which may be a key factor leading to neurotoxicity.

Keywords: Reactive oxygen species; Reactive nitrogen species; Aliphatic, naphthenic, and aromatic hydrocarbons; Rat brain synaptosomes

0006-2952/01/$ – see front matter
PII: S0006-2952(01)00652-9

1. Introduction

High concentrations of hydrocarbon solvents are capable of inducing an acute, reversible narcotic state, but it has been difficult to show chronic irreversible histological changes in the central nervous system. It has been reported that prolonged, low-level exposure to white spirit leads to both behavioral and physiological changes in specific worker populations [1–3]. Chronic inhalation abuse of pure toluene leads to irreversible cerebellar, brainstem, and pyramidal-tract dysfunction [4], and chronic inhalation of toluene-based adhesives can cause irreversible paranoid psychosis, a high incidence of temporal lobe epilepsy, and a decrease in IQ [5].

The toxic effect of white spirit is hypothesized to depend on aromatic compounds. Animal studies have shown changes in global, regional, and subcellular metabolism of neurotransmitters, indicating both acute and long-term effects after exposure to aromatic white spirit [6–8]. Furthermore, aromatic hydrocarbons such as toluene at high concentrations were shown to cause elevation of free radicals and ROS in mammal CNS [9–11], and a 16% loss of neurons was reported in regio inferior (CA3 and CA2) of rats exposed to 1500 ppm toluene for a period of six months [12]. However, several animal studies also indicate that exposure to dearomatized white spirit may lead to brain disorders. Long-lasting electrophysiological changes were observed in rats after six months' exposure to dearomatized white spirit [13]. Edelfors *et al*. [14] demonstrated elevation of $[Ca^{2+}]_i$ in synaptosomes from rats prenatally exposed to dearomatized white spirit, and Lam *et al*. [15] showed that exposure of rats to dearomatized white spirit induced oxidative stress in brain. The white spirit compounds *n*-nonane, TMCH, and TMB were recently shown to elevate production of free radicals and ROS in human neutrophil granulocytes [16]. The cellular mechanisms involved in the production of free radicals in brain tissue after exposure to hydrocarbon solvents are poorly understood. Therefore, the current study focused on the effects of different classes of white spirit C7 and C9 hydrocarbons on oxidative stress in rat brain synaptosomes, and on the cellular mechanisms involved.

Inhalation experiments on rats exposed to the C9 hydrocarbons *n*-nonane, TMCH, and TMB (1000 ppm) showed that the highest concentration in the brain was reached by *n*-nonane (1416 μmol/kg), followed by TMCH (1109 μmol/kg) and TMB (998 μmol/kg) [17]. At low concentrations of the hydrocarbons (100 ppm), TMCH had the highest concentration in the brain (80.5 μmol/kg), followed by *n*-nonane (48.3 μmol/kg) and TMB (38.1 μmol/kg) [18]. Male rats exposed by inhalation to 400 or 800 ppm of dearomatized white spirit for three weeks had a brain concentration of 7.1 and 17.1 mg/kg, respectively [19]. In another inhalation study, male rats were exposed to 400 or 800 ppm aromatic white spirit (containing 20% by vol. aromates) for three weeks. This resulted in a brain concentration of 3.40 and 10.2 mg/kg, respectively [6]. Based on these inhalation experiments, we chose relevant concentrations of the C7 and C9 hydrocarbons, and investigated the effects on production of ROS and RNS in rat brain synaptosomes. MeHg was included as a positive control since several studies have shown the ability of this substance to induce oxidative stress [20–22]. The production of ROS and RNS in the present study was measured as the formation of DCF from non-fluorescent H_2DCF, and thereby elevation of fluorescence. Mechanisms for TMCH-induced elevation of fluorescence were elucidated by use of enzymatic inhibitors, the Ca^{2+}-sensitive probe Fura-2, the Ca^{2+} channel blocker La^{3+}, and the MTP blocker CSA.

2. Materials and methods

2.1. Chemicals

CSA, H_2DCF-DA, BIM, DEDA, *n*-heptane, lanthanum chloride ($LaCl_3$), methanol, L-NAME, *n*-nonane, 4′,5,7-trihydroxyisoflavone (genistein), and toluene were purchased from Sigma-Aldrich. The aminosteroid U73122 was from ICN Biomedicals Inc., TMCH was obtained from Aldrich Chemical Co., and U0126 was purchased from AH Diagnostics AS. Methylcyclohexane and TMB were purchased from ACROS Organics. MeHg was purchased from KEBOLab, and Fura-2 AM was from Molecular Probes. HBSS (containing $CaCl_2 \cdot 2H_2O$ (1.26 mM), KCl (5.37 mM), KH_2PO_4 (0.44 mM), $MgCl_2 \cdot 6H_2O$ (0.49 mM), $MgSO_4 \cdot 7H_2O$ (0.41 mM), NaCl (0.14 M), $NaHCO_3$ (4.17 mM), Na_2HPO_4 (0.34 mM), D-glucose (5.55 mM)) and HEPES buffer were purchased from GIBCO BRL.

2.2. Preparation of rat brain synaptosomes

Each morning, a male Wistar rat (150–200 g) (Møllegaard Breeding Laboratories, Denmark) was decapitated,

* Corresponding author. Tel.: +47-63807858; fax: +47-63807509.
E-mail address: oddvar.myhre@ffi.no (O. Myhre).

Abbreviations: BIM, bisindolylmaleimide; $[Ca^{2+}]_i$, concentration of intracellular calcium; ChAT, cholin acetyltransferase; CSA, cyclosporin A; DCF, 2′,7′-dichlorofluorescein; H_2DCF-DA, 2′,7′-dichlorodihydrofluorescin diacetate; DEDA, dimethyleicosadienoic acid; ERK, extracellular signal-regulated kinases; Fura-2 AM, 5-oxazolecarboxylic acid, 2-(6-(bis(2-((acetyloxy)methoxy)-2-oxoethyl)amino)-5-(2-(bis(2-((acetyloxy)methoxy)-2oxoethyl)amino)-5-methylphenoxy)ethoxy)-2-benzofuranyl)-, (acetyloxy) methyl ester; GABA-T, gamma-aminobutyric acid transaminase; HBSS, Hanks' balanced salt solution; La^{3+}, lanthanum; MAPK, mitogen-activated protein kinase; MeHg, methyl mercury; MEK, extracellular signal-regulated protein kinase; MeOH, methanol; MTP, mitochondrial permeability transition pore; L-NAME, Nω-nitro-L-arginine methyl ester; $NO^{\cdot}$, nitrogen oxide; NOS, $NO^{\cdot}$ synthase; $O_2^{\cdot-}$, superoxide; PLA_2, phospholipase A_2; PKC, protein kinase C; RNS, reactive nitrogen species; ROS, reactive oxygen species; SOD, superoxide dismutase; TMB, 1,2,4-trimethylbenzene; TMCH, 1,2,4-trimethylcyclohexane; and U73122, 1-(6-[17beta-3-methoxyestra- 1,3,5(10)-trien- 17-yl]-aminohexyl)- 1*H*-pyrrole-2,5-dione.

then the cerebral cortex was dissected out, placed on ice-cold 0.32 M sucrose within 30 sec and homogenized in 0.32 M sucrose at 4°. The synaptosomes were prepared in principle as described by Gray and Whittaker [23] and in detail by Voie and Fonnum [21]. In brief, the homogenate was centrifuged at 1000 X *g* for 10 min. The pellet was removed and 1.6 M sucrose was added to the remaining supernatant until the solution reached a sucrose concentration of 0.8 M. The supernatant was than centrifuged at 13,000 X *g* for 30 minutes at 4°, resulting in a myelin-rich supernatant and a pellet (P_2) consisting of free mitochondria covered with synaptosomes. The synaptosome fraction was washed out by adding 1 mL ice-cold 0.32 M sucrose and by gently stirring the suspension. The free mitochondrial fraction, i.e. the remaining pellet of the P_2 fraction, was resuspended by adding 1 mL ice-cold 0.32 M sucrose. The myelin fraction (1 mL) was collected from the supernatant. Thereafter, the three separate fractions were diluted in HEPES-buffered (20 mM) HBSS (pH 7.4). The protein content was determined using the method described by Lowry *et al*. [24]. The synaptosome fraction was diluted to 0.1 mg protein/mL (final concentration in the test solutions) in the HEPES-buffered HBSS. The purity of the density gradient-isolated and the stirring method-isolated synaptosome fractions were determined by measuring the enzyme activity of ChAT, mainly localized in synaptosomes, and GABA-T, mainly localized in the free and synaptosomal mitochondria [25, 26]. The production of ROS by MeHg and TMCH in the synaptosomes isolated by the method described above were compared with synaptosomes isolated from P_2 on a discontinuous Percoll gradient, according to the method described by Dunkley *et al*. [27], and with synaptosomes isolated on a discontinuous sucrose gradient, as described by Voie and Fonnum [21].

2.3. Fluorescence spectroscopy assay

Formation of ROS and RNS in rat brain synaptosomes was determined mainly by the procedure described by LeBel *et al*. [28,29]. In brief, this method is based on the incubation of cells by the probe H_2DCF-DA, which passively diffuses through cellular membranes where the acetates are cleaved by intracellular esterases. Thereafter, the non-fluorescent compound H_2DCF is oxidized by ROS or RNS to the fluorescent compound DCF. The fluorescence was measured by a luminescence spectrometer (LS50B, Perkin Elmer), using an excitation wavelength of 488 nm and an emission wavelength of 525 nm [29].

First, the synaptosome fraction, free mitochondria, and/or the myelin fraction were incubated with H_2DCF-DA (10 μM) in HEPES-buffered (20 mM) HBSS (pH 7.4) with glucose (5.5 mM) at 37° for 15 min. Following centrifugation, the extracellular medium with H_2DCF-DA was exchanged with fresh buffer, and the suspension was gently mixed. Second, the fractions (100 μL) were transferred to 250-μL wells (microtiter plate reader, 96 wells) containing 150 μL buffer with the compounds investigated (MeHg [75 μM], *n*-heptane [25–100 μM], methylcyclohexane [25–100 μM], toluene [0.05–6.5 mM], *n*-nonane [25–100 μM], TMCH [25–100 μM], or TMB [320–1280 μM]). The temperature during the experiments was 37°. The elevation of intraparticular fluorescence was linear with time, and was measured continuously for 90 min.

Mechanisms for hydrocarbon-induced elevation of fluorescence were elucidated by incubation of the above solutions with an enzymatic inhibitor (genistein [100 μM], U0126 [10 μM], BIM [0.25 μM], U73122 [1 μM], DEDA [4 μM], L-NAME [300 μM], La^{3+} [140 μM], or CSA [0.5 μM], all in final concentrations). The control mixtures contained the synaptosomes, the myelin fraction, or the free mitochondria in buffer (control) or synaptosomes with 1% (v/v) MeOH (MeOH control), or an enzymatic inhibitor when added. The concentration of methanol ($\leq$ 1% v/v), the addition of the enzymatic inhibitors, or the addition of the enzymatic inhibitors in combination with MeOH (instead of the test solutions) in the control solutions had only a small, statistically insignificant effect on the measurements compared to the synaptosome control (synaptosomes in HEPES-buffered HBSS).

2.4. Measurement of $[Ca^{2+}]_i$ in synaptosomes

$[Ca^{2+}]_i$ was measured using the fluorescent Ca^{2+}-binding probe Fura-2 [30]. An increase in $[Ca^{2+}]_i$ is indicated by an increase in the fluorescence excitation ratio (I_{340}/I_{380}). The synaptosome fraction was incubated with Fura-2 at 37° for 40 min. Following centrifugation, the extracellular medium with Fura-2 was exchanged with fresh buffer, and the synaptosomes were incubated with the test compounds MeHg or TMCH. The reaction mixture (2 mL) contained (in final concentrations): synaptosomes (0.1 mg/mL) and Fura-2 (10 μM) in HEPES-buffered (20 mM) HBSS (pH 7.4) with 5.5 mM glucose, MeHg (75 μM), or TMCH (100 μM). The control mixtures contained synaptosomes in buffer (synaptosomes in HEPES-buffered HBSS) or synaptosomes with $\leq$1% (v/v) MeOH (MeOH control) instead of the test compounds. The intracellular fluorescence at the emission wavelength of 510 nm was measured continuously for 400 s by a luminescence spectrometer (LS50B, Perkin Elmer). The excitation wavelengths were 340 and 380 nm [31]. The temperature during the experiments was 37°.

2.5. Statistical analysis

Each day, synaptosomes and/or mitochondria were prepared from a rat brain as described, and the effects of the different classes of the hydrocarbon solvents were investigated by comparing the test group (3 parallels) with the control group (also 3 parallels). All the experiments were repeated 3–5 times. The statistical analyses were conducted using two-sided, paired Student's *t*-test.

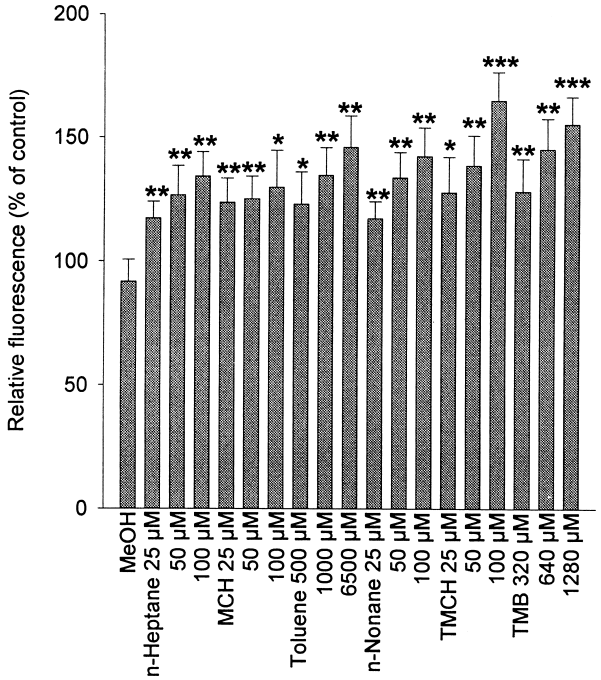

Fig. 1. Relative fluorescence as a measure of ROS and RNS formation in rat brain synaptosome fraction with increasing doses of the test compounds *n*-heptane, methylcyclohexane (MCH), toluene, *n*-nonane, TMCH and TMB. *n*-Heptane, MCH, *n*-nonane, and TMCH showed the strongest stimulatory effect on ROS/RNS production at about 100 μM, toluene at about 6500 μM, and TMB at about 1280 μM. All values are relative to the synaptosome control (synaptosomes in HEPES-buffered HBSS) (100%). Values are means ± SD, N = 5. Two-sided paired Student's *t*-test was performed for the data presented. $*P \leq 0.05$, $**P \leq 0.01$, $***P \leq 0.001$.

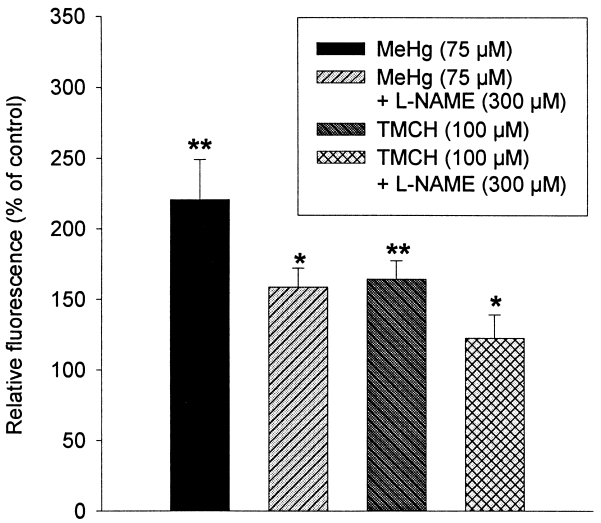

Fig. 2. Relative fluorescence as a measure of ROS and RNS formation in the rat brain synaptosome fraction during exposure to MeHg with and without the NOS inhibitor L-NAME (N = 4), and to TMCH in the presence and absence of L-NAME (N = 5). The experiments including L-NAME are relative to the L-NAME control (synaptosomes in HEPES-buffered HBSS with L-NAME), while the experiments without an inhibitor are relative to the synaptosome control (synaptosomes in HEPES-buffered HBSS) (100%). The experiments with the inhibitor are significantly different from those without the inhibitor, indicating involvement of $NO^{\cdot}$ in the oxidation of the DCFH probe after stimulation with MeHg and TMCH. Values are means ± SD. Two-sided paired Student's *t*-test was performed for the data presented. $*P \leq 0.05$, $**P \leq 0.01$.

3. Results

3.1. Effects of the C7 and C9 hydrocarbons n-*heptane, methylcyclohexane, toluene,* n-*nonane, TMCH, and TMB on formation of ROS and RNS in rat brain synaptosomes*

The rat brain synaptosome fraction was exposed to different concentrations of the test compounds *n*-heptane, methylcyclohexane, toluene, *n*-nonane, TMCH, and TMB, and the oxidation of H_2DCF to DCF was used as a measure of the formation of ROS and RNS (Fig. 1). The hydrocarbons increased fluorescence in a concentration-dependent manner, and there was a statistically significant difference ($P \leq 0.05$) between the control and the organic solvents *n*-heptane (25 μM), methylcyclohexane (25 μM), toluene (500 μM), *n*-nonane (25 μM), TMCH (25 μM), and TMB (320 μM) (Fig. 1). These concentrations corresponded to about half of the dose that gave the highest net responses for the hydrocarbons in this test system compared to the synaptosome control (synaptosomes in HEPES-buffered HBSS).

The potential for ROS and RNS formation by MeHg and TMCH in the synaptosome fraction isolated by the method described was compared with synaptosomes isolated from P_2 on a discontinuous Percoll gradient [27] and with synaptosomes isolated on a discontinuous sucrose gradient [21]. The experiments showed that there were no statistically significant differences between the DCF fluorescence stimulated by MeHg (75 μM) or TMCH (100 μM) in these three synaptosome preparations (not shown). The purity of the applied synaptosomes and the free mitochondria was radiochemically assayed by measuring the enzyme activity of ChAT and GABA-T [25,26]. Both the stirring-isolated synaptosome fraction and the density gradient-isolated synaptosomes (see Materials and Methods) contained about 70% of ChAT and 30% GABA-T, while the corresponding mitochondrial fractions contained about 30% ChAT and 70% GABA-T.

Formation of RNS was shown by preincubating the synaptosomes with the nNOS inhibitor L-NAME [32]. This resulted in a 51% and 65% decrease in the DCF fluorescence after stimulation with MeHg and TMCH, respectively (Fig. 2). The response after stimulation of both the synaptosome and mitochondrial fractions was stronger after treatment with MeHg (75 μM) than with TMCH (100 μM) (Fig. 3). The myelin fraction did not respond to MeHg or TMCH.

3.2. The involvement of Ca^{2+} and the MTP

Addition of MeHg or TMCH to the synaptosome fraction after preincubation with the Ca^{2+}-sensitive probe Fura-2

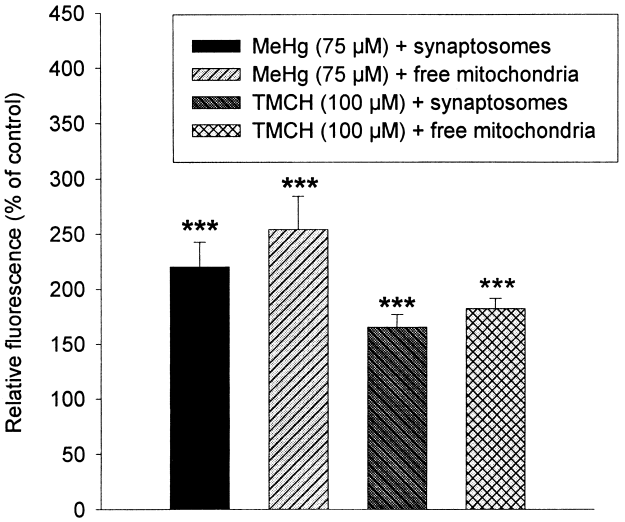

Fig. 3. Relative fluorescence as a measure of ROS and/or RNS formation in the synaptosome fraction and free mitochondria during exposure to MeHg and TMCH. All values are relative to the synaptosome or mitochondria control (synaptosomes or mitochondria in HEPES-buffered HBSS) (100%). The results indicate formation of ROS after stimulation of mitochondria with MeHg and TMCH. Values are means ± SD, N = 5. Two-sided paired Student's *t*-test was performed for the data presented. $***P \leq 0.001$.

resulted in elevation of $[Ca^{2+}]_i$, shown as an increased fluorescence exitation ratio (I_{340}/I_{380}) (Fig. 4). Methanol (1% v/v) did not lead to influx of Ca^{2+} (not shown). To further investigate the contribution of Ca^{2+} channels to ROS/RNS formation, La^{3+} was used to block the Ca^{2+} channels [33]. La^{3+} lowered the DCF fluorescence after

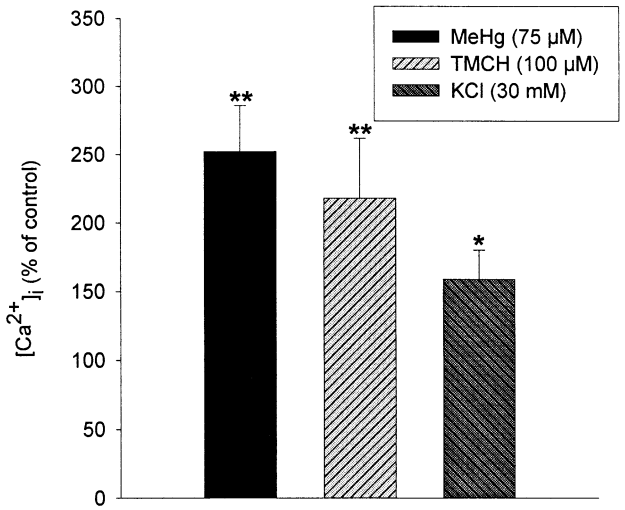

Fig. 4. Relative $[Ca^{2+}]_i$ in Fura-2-loaded synaptosome fraction after exposure to MeHg, TMCH, and potassium chloride (KCl). Relative $[Ca^{2+}]_i$ was assayed in the synaptosome suspension over a 400-sec period. All values are relative to the synaptosome control (synaptosomes in HEPES-buffered HBSS) (100%). Values are means ± SD, N = 3. Two-sided paired Student's *t*-test was performed for the data presented. $P \leq 0.05$, $**P \leq 0.01$.

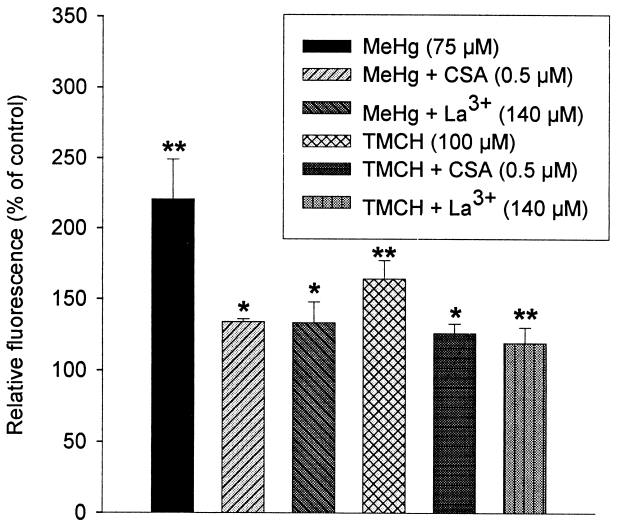

Fig. 5. Relative fluorescence as a measure of ROS and RNS formation in rat brain synaptosome fraction during exposure to MeHg (N = 4) and TMCH (N = 5) in the presence and absence of the MTP inhibitor CSA and La^{3+}, which blocks the voltage-sensitive Ca^{2+} channels. The experiments in the prescence of MTP or La^{3+} are relative to the respective controls (synaptosomes in HEPES-buffered HBSS with MTP or La^{3+}), while the experiments in the absence of the inhibitors are relative to the synaptosome control (synaptosomes in HEPES-buffered HBSS) (100%). The experiments with the inhibitors are significantly different from those without the inhibitors, indicating that the DCF fluorescence is dependent on both the MTP and Ca^{2+} influx through voltage-sensitive Ca^{2+} channels after stimulation with MeHg and TMCH. Values are means ± SD. Two-sided paired Student's *t*-test was performed for the data presented. $*P \leq 0.05$, $**P \leq 0.01$.

stimulation with MeHg and TMCH by 72% and 70%, respectively (Fig. 5). Inhibition of the MTP by CSA [34] lowered the MeHg- and TMCH-stimulated DCF fluorescence by 72% and 59%, respectively (Fig. 5).

3.3. The involvement of tyrosine kinase and the MAPK pathway

Preincubation of the synaptosomes with the protein tyrosine kinase inhibitor genistein [35] reduced the DCF fluorescence formation induced by MeHg and TMCH by 85% and 91%, respectively (Fig. 6), while U0126, which inhibits the MAPK kinase family members MEK-1 and MEK-2 [36,37], led to a lowering of the fluorescence by 62% and 63%, respectively (Fig. 6).

3.4. The involvement of PKC, phospholipase C and phospholipase A_2

Since phospholipases and PKC are known to be involved in the production of free radicals in some tissues [16,21,38], the synaptosome fraction was preincubated with the PKC inhibitor BIM [39], the phospholipase C inhibitor U73122 [40,41], and the PLA_2 inhibitor DEDA [42]. BIM reduced the DCF fluorescence produced by MeHg and TMCH by

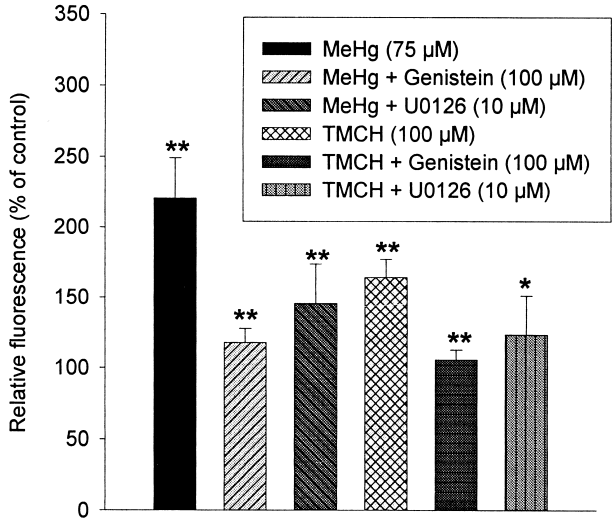

Fig. 6. Relative fluorescence as a measure of ROS and RNS formation in rat brain synaptosome fraction during exposure to MeHg (N = 4) and TMCH (N = 5) in the presence and absence of the protein tyrosine kinase inhibitor genistein and the compound U0126, which inhibits the mitogen-activated protein kinase kinase (MAPKK) family members MEK-1 and MEK-2. The experiments in the prescence of the inhibitors are relative to the respective controls (synaptosomes in HEPES-buffered HBSS with genistein or U0126), while the experiments in the absence of the inhibitors are relative to the synaptosome control (synaptosomes in HEPES-buffered HBSS) (100%). The experiments with the inhibitors are significantly different from those without the inhibitors, indicating that the DCF fluorescence is dependent on protein tyrosin kinases and the ERK type of MAPKs. Values are means ± SD. Two-sided paired Student's *t*-test was performed for the data presented. $*P \leq 0.05$, $**P \leq 0.01$.

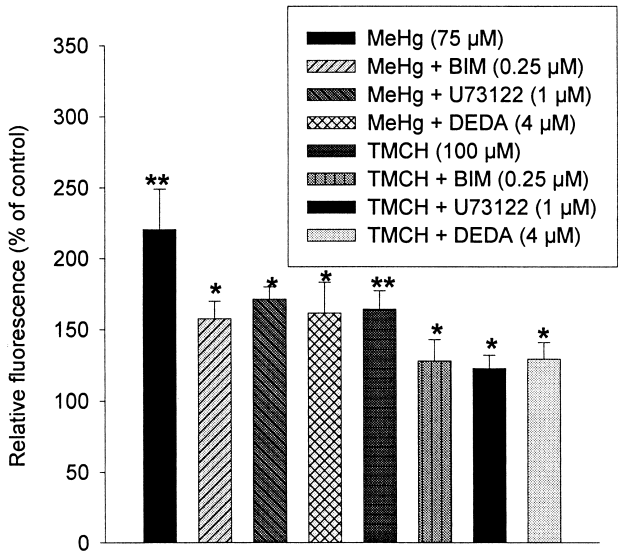

Fig. 7. Relative fluorescence as a measure of ROS and RNS formation in rat brain synaptosome fraction during exposure to MeHg and TMCH in the presence and absence of the PKC inhibitor BIM, the phospholipase C inhibitor U73122, and the PLA_2 inhibitor DEDA. The experiments in the prescence of the inhibitors are relative to the respective controls (synaptosomes in HEPES-buffered HBSS with BIM, U73122, or DEDA), while the experiments in the absence of the inhibitors are relative to the synaptosome control (synaptosomes in HEPES-buffered HBSS) (100%). The experiments with the inhibitors are significantly different from those without the inhibitors, indicating that the DCF fluorescence is dependent on PKC, phospholipase C, and phospholipase A_2. Values are means ± SD. Two-sided paired Student's *t*-test was performed for the data presented. $*P \leq 0.05$, $**P \leq 0.01$.

52% and 56%, U73122 reduced it by 49% and 64%, and DEDA by 49% and 54%, respectively (Fig. 7).

4. Discussion

4.1. Effects of the C7 and C9 hydrocarbons n-*heptane, methylcyclohexane, toluene,* n-*nonane, TMCH and TMB on formation of ROS and RNS in rat brain synaptosomes*

Our experiments show that C7 and C9 aliphatic, naphthenic, and aromatic hydrocarbons stimulate production of ROS and RNS in rat brain synaptosomes. Of the hydrocarbons tested, TMCH was the most potent stimulator, followed by TMB, toluene, *n*-nonane, methylcyclohexane, and *n*-heptane, respectively (Fig. 1). The aliphatic and naphthenic hydrocarbons *n*-heptane, methylcyclohexane, *n*-nonane, and TMCH induced formation of ROS and RNS in a concentration found in rat brains after inhalation of a low concentration of organic solvents (100 ppm) whereas the aromatic compounds toluene and TMB are active in a concentration relevant to an acute high exposure (1000 ppm) [17,18]. The concentrations of the solvents chosen in our study are also comparable to rat brain concentrations after inhalation of aromatic and dearomatic white spirit mixtures [6,19]. The water solubility of *n*-heptane, *n*-nonane, methylcyclohexane, TMCH, toluene, and TMB is approximately 75 μM, 5 μM, 255 μM, 15 μM, 6.5 mM, and 625 μM, respectively [43]. The elevation of fluorescence observed when exceeding these concentrations is probably the result of mixing the synaptosomes with the buffer containing the hydrocarbons. This will lead to accumulation of these fat-soluble substances in the membranes, and thereby formation of ROS.

The radiochemical assay shows that the purity of the synaptosome fractions used in this work (both the density gradient-purified and the stirring-purified) was relatively high, with little contamination of free mitochondria, while the mitochondrial fractions contained some synaptosomes. This indicates that the fast and simple method for isolating synaptosomes presented here is suitable for measuring ROS in the synaptosome fraction. Furthermore, there were no statistically significant differences in the results obtained after MeHg- and TMCH-induced stimulation of the synaptosomes isolated from a discontinuous Percoll gradient, a discontinuous sucrose gradient, and by the present method.

Formation of $NO^{\cdot}$ was demonstrated by reduced DCF fluorescence obtained after preincubation of the synaptosome fraction with L-NAME, an nNOS inhibitor [32], prior to stimulation with MeHg and TMCH (Fig. 2). Radicals

such as $NO^{\cdot}$ and $O_2^{\cdot -}$ have little propensity to react with non-radical biomolecules, but the combination of $NO^{\cdot}$ and $O_2^{\cdot -}$ results in rapid generation of the highly reactive molecule peroxynitrite [44]. Because $NO^{\cdot}$ reacts with $O_2^{\cdot -}$ threefold faster than SOD, $NO^{\cdot}$ is the only known biomolecule capable of outcompeting SOD for available $O_2^{\cdot -}$ [45]. Several studies have reported that H_2DCF is much more sensitive to peroxynitrite oxidation than to oxidation by H_2O_2, $O_2^{\cdot -}$, and $NO^{\cdot}$ [46–48]. This indicates that peroxynitrite may be an important source of the MeHg- and TMCH-induced oxidative stress in our experiments, and could contribute to about half of the increase in the DCF fluorescence (Fig. 2).

Incubation of the synaptosome and free mitochondrial fractions with the positive control MeHg resulted in a larger elevation of ROS than did treatment with TMCH (Fig. 2), indicating that MeHg may have higher ROS-forming potential than the hydrocarbon solvent. The experiments with the mitochondria were conducted in an extracellular environment, with a relatively high Ca^{2+} ion concentration, to imitate high transient Ca^{2+} levels in the cytosol. High $[Ca^{2+}]_i$ in cytosol (0.5–5 μM) is followed by fast Ca^{2+} uptake by the mitochondria. In addition to elevated Ca^{2+}, opening of the MTP and thereby mitochondrial membrane potential collapse requires several stimuli, such as agents oxidizing thiol (−SH) groups and/or formation of ROS [49–51]. In our experiments, we used extracellular concentrations of Na^+ and K^+. Even under these conditions, the effects of MeHg and TMCH on ROS formation in the mitochondria were clearly demonstrated. Incubation of the myelin fraction with MeHg or TMCH did not lead to an elevation of the DCF fluorescence (Fig. 3). This indicates that there were no synaptosomes or free mitochondria in the myelin fraction.

The neurotoxic compound MeHg was included as a positive control, since MeHg is known to stimulate formation of ROS in synaptosomes and in the hypothalamic neural cell line GT1-7, and to decrease the level of GSH [20–22]. Furthermore, MeHg has been shown to increase $[Ca^{2+}]_i$ and induce the production of inositol phosphate in cerebellar granule cells [52], and to disrupt Ca^{2+} homeostasis within isolated synaptosomes [53,54].

4.2. The involvement of Ca^{2+}

Exposure to hydrocarbon solvents such as white spirit and toluene is well known to elevate intraparticular Ca^{2+} in rat brain synaptosomes [55–57]. Our experiments with the synaptosomes incubated with the Ca^{2+}-sensitive probe Fura-2 (Fig. 4) showed an elevation of $[Ca^{2+}]_i$ after exposure to both MeHg and TMCH, indicating a possible Ca^{2+}-dependent mechanism for ROS/RNS formation. This was further investigated by using La^{3+} to block voltage-sensitive Ca^{2+} channels as well as store-operated ion channels [33]. La^{3+} caused a significant lowering of the ROS/RNS production after stimulation with MeHg and TMCH (Fig. 5). In this respect, it should be mentioned that genistein, the tyrosine kinase inhibitor, also inactivates P/Q calcium channels in neurons [58] (Fig. 6).

4.3. The MTP and ROS/RNS formation

The MTP, a voltage-dependent mitochondrial channel, is known to play an important role in the pathways leading to ROS production and cell death [59]. Several stimuli such as high mitochondrial matrix Ca^{2+} load, dithiol oxidation, membrane depolarization, and ROS trigger the assembly and opening of the MTP, leading to formation of ROS. This opening can be inhibited by CSA [60,61]. Incubation of the synaptosome fraction with CSA in our experiments led to a significant reduction in ROS/RNS formation after stimulation with MeHg and TMCH (Fig. 5).

4.4. The involvement of tyrosine kinase and the MAPK pathway

ERK1/2 are classical members of the MAPK superfamily, and are thought to be activated via the Ras/Raf/MEK/ERK cascade [62–65]. Activation of ERK1/2 has been found in some excitotoxic-associated events such as Alzheimer's disease, seizure, and ischemia [66–69], and is involved in elevation of free radicals in different tissue preparations, e.g. in Ca^{2+}-dependent excitotoxicity in cultured rat cortical neurons [70], in glutamate-induced oxidative toxicity in the HT22 hippocampal cell line and immature primary cortical neuron cultures [71], and in the activation of PLA_2 in neutrophils [72]. In order to investigate the role of the MAPK-signaling pathway in TMCH-stimulated ROS/RNS formation, the synaptosome fraction was preincubated with the protein tyrosine kinase inhibitor genistein [35] and the MEK1/2 inhibitor U0126 [36,37], which lowered the production of ROS (Fig. 6). Genistein is reported to block tyrosine phosphorylation of PLCγ in the rat dendate gyrus [73], to inactivate P/Q calcium channels in neurons [58], and to inhibit activation of PLA_2 and [^{3}H]arachidonic acid release in rat hepatocytes [74]. The upstream activator of MEK1/2, Raf-1, can be activated by protein kinase C [75], indicating cross-talk between the MAPK- and PKC-signaling pathways. The MAPK cascade can also be activated by influx of extracellular Ca^{2+} [71]. From our experiments with the enzyme inhibitors and the stimulators MeHg and TMCH, we observed Ca^{2+} influx, which leads to activation of both the MAPK pathway and Ca^{2+}-dependent PKC (Figs. 6 and 7). This Ca^{2+} influx will also activate PLA_2 and lead to opening of the MTP, and thereby production of ROS.

4.5. The involvement of PKC, phospholipase C, and phospholipase A_2

There are several links between PKC and the phospholipases for production of ROS. Such links have been clearly

demonstrated in human granulocytes [16,38]. It was therefore of importance to see if the same system is present in synaptosomes. Inhibition of PKC with BIM [39] reduced ROS formation in the synaptosomes after stimulation with MeHg and TMCH (Fig. 7). Treatment of the synaptosome fraction with U73122, a phospholipase C inhibitor [40,41], also reduced DCF fluorescence after stimulation with MeHg and TMCH (Fig. 7). Previously, we found a similar effect in human neutrophils [16]. Phospholipase C is known to hydrolyze phosphatidylinositol-4,5-bisphosphate, generating inositol 1,4,5-trisphosphate, which stimulates Ca^{2+} release from intracellular compartments, and diacylglycerol, which activates PKC. Furthermore, it has been reported that inhibition of phospholipase C by U73122 prevents glutamate neurotoxicity in primary cultures of cerebellar neurons [76].

Incubation of the synaptosome fraction with DEDA, a PLA_2 inhibitor [42], reduced fluorescence after stimulation with MeHg and TMCH (Fig. 7). This is in agreement with earlier findings in human neutrophils [77]. The activity of PLA_2 has been reported to be enhanced by MAPK and/or PKC [78], in addition to Ca^{2+} [79]. PLA_2 activated by Ca^{2+} influx is known to give rise to ROS in cerebellar granule cells exposed to glutamate [80]. Simultaneous incubation of the synaptosome fraction with CSA, DEDA, and L-NAME in combination with TMCH completely abolished the DCF fluorescence (not shown), which confirms that the main sources of ROS/RNS production were the mitochondria, PLA_2, and formation of peroxynitrite after the reaction between NO and $O_2^{\cdot -}$.

In summary, C7 and C9 aliphatic, naphthenic, and aromatic hydrocarbons stimulated formation of ROS in rat brain synaptosomes. The naphthenic hydrocarbon TMCH was selected for mechanistic studies, and the results showed that the formation of ROS and RNS was dependent on Ca^{2+} activation of PLA_2, nNOS, and an increased transition permeability of the MTP. The increased formation of $O_2^{\cdot -}$ may lead to formation of peroxynitrite after combination with $NO^{\cdot}$. The TMCH-stimulated activation of the PKC and MAPK pathways is involved in both the activation of PLA_2 and in mitochondrial dysfunction. It may appear a paradox that the efforts of converting aromatic hydrocarbons to the corresponding naphthenic compounds may result in higher accumulation in brain tissue and stronger potential for production of damaging free radicals in nerve cell terminals.

The elevation of ROS in synaptosomes and mitochondria observed in the present work may result in damage to receptors, enzymes, and ion pumps. ROS may also interfere with nucleic acids and thus generate mutations or initiate lipid peroxidation. The importance of long-lasting, abnormally high production of ROS are evident in neurodegenerative conditions such as Alzheimer's disease, Parkinson's disease, and amyotrophic lateral sclerosis. Furthermore, it is possible that effects similar to those studied in this work may operate *in vivo* after exposure to hydrocarbon solvents, thereby leading to disturbances of signaling pathways and critical cellular events in neural tissue. This may explain some of the neurotoxicity observed in man and animals after hydrocarbon solvent exposure.

References

[1] Mikkelsen S, Jorgensen M, Browne E, Gyldensted C. Mixed solvent exposure and organic brain damage. A study of painters. Acta Neurol Scand Suppl 1988;118:1–143.
[2] Arlien-Søborg P, Hansen L, Ladefoged O, Simonsen L. Report on a conference on organic solvents and the nervous system. Neurotoxicol Teratol 1992;14:81–2.
[3] Triebig G, Barocka A, Erbguth F, Holl R, Lang C, Lehrl S, Rechlin T, Weidenhammer W, Weltle D. Neurotoxicity of solvent mixtures in spray painters. II. Neurologic, psychiatric, psychological, and neuroradiologic findings. Int Arch Occup Environ Health 1992;64:361–72.
[4] Spencer PS, Schaumburg HH. Organic solvent neurotoxicity. Facts and research needs. Scand J Work Environ Health 1985;11:53–60.
[5] Byrne A, Kirby B, Zibin T, Ensminger S. Psychiatric and neurological effects of chronic solvent abuse. Can J Psychiatry 1991;36:735–8.
[6] Lam HR, Löf A, Ladefoged O. Brain concentrations of white spirit components and neurotransmitters following a three week inhalation exposure of rats. Pharmacol Toxicol 1992;70:394–6.
[7] Lam HR, Østergaard G, Ladefoged O. Three weeks' and six months' exposure to aromatic white spirit affect synaptosomal neurochemistry in rats. Toxicol Lett 1995;80:39–48.
[8] Østergaard G, Lam HR, Ladefoged O, Arlien-Søborg P. Effects of six months' white spirit inhalation exposure in adult and old rats. Pharmacol Toxicol 1993;72:34–9.
[9] Mattia CJ, LeBel CP, Bondy S. Effects of toluene and its metabolites on cerebral reactive oxygen species generation. Biochem Pharmacol 1991;42:879–82.
[10] Mattia CJ, Adams JD, Bondy SC. Free radical induction in the brain and liver by products of toluene catabolism. Biochem Pharmacol 1993;46:103–10.
[11] Mattia CJ, Ali SF, Bondy SC. Toluene-induced oxidative stress in several brain regions and other organs. Mol Chem Neuropathol 1993;18:313–28.
[12] Korbo L, Ladefoged O, Lam HR, Østergaard G, West MJ, Arlien-Søborg P. Neuronal loss in hippocampus in rats exposed to toluene. Neurotoxicology 1996;17:359–66.
[13] Lund SP, Simonsen L, Hass U, Ladefoged O, Lam HR, Østergaard G. Dearomatised white spirit inhalation exposure causes long-lasting neurophysiological changes in rats. Neurotoxicol Teratol 1996;18:67–76.
[14] Edelfors S, Hass U, Ravn-Jonsen A. The effect of *in vitro* exposure to white spirit on $[Ca^{2+}]_i$ in synaptosomes from rats exposed prenatally to white spirit. Pharmacol Toxicol 1999;84:197–200.
[15] Lam HR, Østergaard G, Guo SX, Ladefoged O, Bondy SC. Three weeks' exposure of rats to dearomatised white spirit modifies indices of oxidative stress in brain, kidney, and liver. Biochem Pharmacol 1994;47:651–7.
[16] Myhre O, Vestad TA, Sagstuen E, Aarnes H, Fonnum F. The effects of aliphatic (*n*-nonane), naphthenic (1,2,4-trimethylcyclohexane) and aromatic (1,2,4-trimethylbenzene) hydrocarbons on respiratory burst in human neutrophil granulocytes. Toxicol Appl Pharmacol 2000;167:222–30.
[17] Zahlsen K, Nilsen AM, Eide I, Nilsen OG. Accumulation and distribution of aliphatic (*n*-nonane), aromatic (1,2,4-tritoluene) and naphthenic (1,2,4-trimethylcyclohexane) hydrocarbons in the rat after repeated inhalation. Pharmacol Toxicol 1990;67:436–40.
[18] Zahlsen K, Eide I, Nilsen AM, Nilsen OG. Inhalation kinetics of C6 to C10 aliphatic, aromatic and naphthenic hydrocarbons in rat after repeated exposures. Pharmacol Toxicol 1992;71:144–9.

[19] Löf A, Lam HR, Gullstrand E, Østergaard G, Ladefoged O. Distribution of dearomatised white spirit in brain, blood, and fat tissue after repeated exposure of rats. Pharmacol Toxicol 1999;85:92–7.
[20] Ali SF, LeBel CP, Bondy SC. Reactive oxygen species formation as a biomarker of methylmercury and trimethyltin neurotoxicity. Neurotoxicology 1992;13:637–48.
[21] Voie OA, Fonnum F. Effect of polychlorinated biphenyls on production of reactive oxygen species (ROS) in rat synaptosomes. Arch Toxicol 2000;73:588–93.
[22] Sarafian TA, Vartavarian L, Kane DJ, Bredesen DE, Verity MA. bcl-2 expression decreases methyl mercury-induced free-radical generation and cell killing in a neural cell line. Toxicol Lett 1994;74: 149–55.
[23] Gray E, Whittaker VP. The isolation of nerve endings from brain: an electron-microscopic study of cell fragments derived by homogenization and centrifugation. J Anat 1962;96:79–88.
[24] Lowry OH, Rosenbrough NJ, Farr AL, Randall RJ. Protein measurement with the folin phenol reagent. J Biol Chem 1951;193:265–75.
[25] Fonnum F. A rapid radiochemical method for the determination of choline acetyltransferase. J Neurochem 1975;24:407–9.
[26] Sterri SH, Fonnum F. Acetyl-CoA synthesizing enzymes in cholinergic nerve terminals. J Neurochem 1980;35:249–54.
[27] Dunkley PR, Jarvie PE, Heath JW, Kidd GJ, Rostas JA. A rapid method for isolation of synaptosomes on Percoll gradients. Brain Res 1986;372:115–29.
[28] LeBel CP, Ali SF, McKee M, Bondy SC. Organometal-induced increases in oxygen reactive species: the potential of 2′,7′-dichlorofluorescin diacetate as an index of neurotoxic damage. Toxicol Appl Pharmacol 1990;104:17–24.
[29] LeBel CP, Ischiropoulos H, Bondy SC. Evaluation of the probe 2′,7′-dichlorofluorescin as an indicator of reactive oxygen species formation and oxidative stress. Chem Res Toxicol 1992;5:227–31.
[30] Grynkiewicz G, Poenie M, Tsien RY. A new generation of Ca^{2+} indicators with greatly improved fluorescence properties. J Biol Chem 1985;260:3440–50.
[31] Tsien RY, Rink TJ, Poenie M. Measurement of cytosolic free Ca^{2+} in individual small cells using fluorescence microscopy with dual excitation wavelengths. Cell Calcium 1985;6:145–57.
[32] Moncada S, Palmer RM, Higgs EA. Nitric oxide: physiology, pathophysiology, and pharmacology. Pharmacol Rev 1991;43:109–42.
[33] Marley PD, O'Farrell M, Bales PJ. Selective effects of metal ions on catecholamine secretion. Meeting abstract. 10th international symposium on chromaffin cell biology, Bergen, Norway, 1999.
[34] Baysal K, Brierly GP, Novgorodov S, Jung DW. Regulation of the mitochondrial Na^{2+}/Ca^{2+} antiport by matrix pH. Arch Biochem Biophys 1991;291:383–9.
[35] O'Dell TJ, Kandel ER, Grant SG. Long-term potentiation in the hippocampus is blocked by tyrosine kinase inhibitors. Nature 1991; 353:558–60.
[36] Duncia JV, Santella JB, Higley CA, Pitts WJ, Wityak J, Frietze WE, Rankin FW, Sun JH, Earl RA, Tabaka AC, Teleha CA, Blom KF, Favata MF, Manos EJ, Daulerio AJ, Stradley DA, Horiuchi K, Copeland RA, Scherle PA, Trzaskos JM, Magolda RL, Trainor GL, Wexler RR, Hobbs FW, Olson RE. MEK inhibitors: the chemistry and biological activity of U0126, its analogs, and cyclization products. Bioorg Med Chem Lett 1998;8:2839–44.
[37] Favata MF, Horiuchi KY, Manos EJ, Daulerio AJ, Stradley DA, Feeser WS, Van Dyk DE, Pitts WJ, Earl RA, Hobbs F, Copeland RA, Magolda RL, Scherle PA, Trzaskos JM. Identification of a novel inhibitor of mitogen-activated protein kinase kinase. J Biol Chem 1998;273:18623–32.
[38] Voie OA, Wiik P, Fonnum F. Ortho-substituted polychlorinated biphenyls activate respiratory burst measured as luminol-amplified chemoluminescence in human granulocytes. Toxicol Appl Pharmacol 1998;150:369–75.
[39] Bit RA, Davis PD, Elliott LH, Harris W, Hill CH, Keech E, Kumar H, Lawton G, Maw A, Nixon JS, Vesey DR, Wadsworth J, Wilkinson SE. Inhibitors of protein kinase C. 3. Potent and highly selective bisindolylmaleimides by conformational restriction. J Med Chem 1993;36:21–9.
[40] Bleasdale JE, Thakur NR, Gremban RS, Bundy GL, Fitzpatrick FA, Smith RJ, Bunting S. Selective inhibition of receptor-coupled phospholipase C-dependent processes in human platelets and polymorphonuclear neutrophils. J Pharmacol Exp Ther 1990;255:756–68.
[41] Smith RJ, Sam LM, Justen JM, Bundy GL, Bala GA, Bleasdale JE. Receptor-coupled signal transduction in human polymorphonuclear neutrophils: effects of a novel inhibitor of phospholipase C-dependent processes on cell responsiveness. J Pharmacol Exp Ther 1990;253: 688–97.
[42] Cohen N, Weber G, Banner BL, Welton AF, Hope WC, Crowley H, Anderson WA, Simko BA, O'Donnell M, Coffey JW. Analogs of arachidonic acid methylated at C-7 and C-10 as inhibitors of leukotriene biosynthesis. Prostaglandins 1984;27:553–62.
[43] Dannenfelser RM, Yalkowsky SH. Database of aqueous solubility for organic nonelectrolytes. Sci Tot Environ 1991;109:625–8.
[44] Huie RE, Padmaja S. The reaction of NO with superoxide. Free Radic Res Commun 1993;18:18195–9.
[45] Torreilles F, Salman-Tabcheh S, Guerin M, Torreilles J. Neurodegenerative disorders: the role of peroxynitrite. Brain Res 1999;30: 153–63.
[46] Crow JP. Dichlorodihydrofluorescein and dihydrorhodamine 123 are sensitive indicators of peroxynitrite *in vitro*: implications for intracellular measurement of reactive nitrogen and oxygen species. Nitric Oxide 1997;1:145–57.
[47] Possel H, Noack H, Augustin W, Keilhoff G, Wolf G. 2,7-Dihydrodichlorofluorescein diacetate as a fluorescent marker for peroxynitrite formation. FEBS Lett 1997;416:175–8.
[48] Wang H, Joseph JA. Quantifying cellular oxidative stress by dichlorofluorescein assay using microplate reader. Free Radic Biol Med 1999;27:612–6.
[49] Packer MA, Murphy MP. Peroxynitrite formed by simultaneous nitric oxide and superoxide generation causes cyclosporin-A-sensitive mitochondrial calcium efflux and depolarisation. Eur J Biochem 1995; 234:231–9.
[50] Kristal BS, Park BK, Yu BP. 4-Hydroxyhexenal is a potent inducer of the mitochondrial permeability transition. J Biol Chem 1996;271: 6033–8.
[51] Bernardi P, Petronilli V. The permeability transition pore as a mitochondrial calcium release channel: a critical appraisal. J Bioenerg Biomembr 1996;28:131–8.
[52] Sarafian TA. Methylmercury increases intracellular Ca^{2+} and inositol phosphate levels in cultured cerebellar granule neurons. J Neurochem 1993;61:648–57.
[53] Komulainen H, Bondy SC. Increased free intrasynaptosomal Ca^{2+} by neurotoxic organometals: distinctive mechanisms. Toxicol Appl Pharmacol 1987;88:77–86.
[54] Kauppinen RA, Komulainen H, Taipale H. Cellular mechanisms underlying the increase in cytosolic free calcium concentration induced by methylmercury in cerebrocortical synaptosomes from guinea pig. J Pharmacol Exp Ther 1989;248:1248–54.
[55] Edelfors S, Ravn-Jonsen A. Effects of simultaneous ethanol and toluene exposure on nerve cells measured by changes in synaptosomal calcium uptake and (Ca^{2+}/Mg^{2+})-ATPase activity. Pharmacol Toxicol 1991;69:90–5.
[56] von Euler G, Fuxe K, Bondy SC. Ganglioside GM1 prevents and reverses toluene-induced increases in membrane fluidity and calcium levels in rat brain synaptosomes. Brain Res 1990;508:210–4.
[57] Edelfors S, Ravn-Jonsen A. Calcium uptake in brain synaptosomes from rats exposed to daily toluene for up to 80 weeks. Pharmacol Toxicol 1987;61:305–7.
[58] Potier B, Rovira C, Protein tyrosine kinase inhibitors reduce high-voltage activating calcium currents in CA1 pyramidal neurones from rat hippocampal slices. Brain Res 1999;816:587–97.

[59] Bernardi P. The permeability transition pore. Control points of a cyclosporin A-sensitive mitochondrial channel involved in cell death. Biochim Biophys Acta 1996;1275:5–9.
[60] Petronilli V, Nicolli A, Costantini P, Colonna R, Bernardi P. Regulation of the permeability transition pore, a voltage-dependent mitochondrial channel inhibited by cyclosporin A. Biochim Biophys Acta 1994;1187:255–9.
[61] Petronilli V, Cola C, Massari S, Colonna R, Bernardi P. Physiological effectors modify voltage sensing by the cyclosporin A-sensitive permeability transition pore of mitochondria. J Biol Chem 1993;268: 21939–45.
[62] Nakielny S, Cohen P, Wu J, Sturgill T. MAP kinase activator from insulin-stimulated skeletal muscle is a protein threonine/tyrosine kinase. EMBO J 1992;11:2123–9.
[63] Seger R, Ahn NG, Posada J, Munar ES, Jensen AM, Cooper JA, Cobb MH, Krebs EG. Purification and characterization of mitogen-activated protein kinase activator(s) from epidermal growth factor-stimulated A431 cells. J Biol Chem 1992;267:14373–81.
[64] Davis RJ. The mitogen-activated protein kinase signal transduction pathway. J Biol Chem 1993;268:14553–6.
[65] Fukunaga K, Miyamoto E. Role of MAP kinase in neurons. Mol Neurobiol 1998;16:79–95.
[66] Arendt T, Holzer M, Grossmann A, Zedlick D, Bruckner MK. Increased expression and subcellular translocation of the mitogen activated protein kinase kinase and mitogen-activated protein kinase in Alzheimer's disease. Neuroscience 1995;68:5–18.
[67] Perry G, Roder H, Nunomura A, Takeda A, Friedlich AL, Zhu X, Raina AK, Holbrook N, Siedlak SL, Harris PL, Smith MA. Activation of neuronal extracellular receptor kinase (ERK) in Alzheimer disease links oxidative stress to abnormal phosphorylation. Neuroreport 1999;10:2411–5.
[68] Gass P, Kiessling M, Bading H. Regionally selective stimulation of mitogen activated protein (MAP) kinase tyrosine phosphorylation after generalized seizures in the rat brain. Neurosci Lett 1993;162: 39–42.
[69] Hu BR, Wieloch T. Tyrosine phosphorylation and activation of mitogen-activated protein kinase in the rat brain following transient cerebral ischemia. J Neurochem 1994;62:1357–67.
[70] Jiang Q, Gu Z, Zhang G, Jing G. Diphosphorylation and involvement of extracellular signal-regulated kinases (ERK1/2) in glutamate-induced apoptotic-like death in cultured rat cortical neurons. Brain Res 2000;857:71–7.
[71] Stanciu M, Wang Y, Kentor R, Burke N, Watkins S, Kress G, Reynolds I, Klann E, Angiolieri MR, Johnson JW, DeFranco DB. Persistent activation of ERK contributes to glutamate-induced oxidative toxicity in a neuronal cell line and primary cortical neuron cultures. J Biol Chem 2000;275:12200–6.
[72] Olivero J, Ganey PE. Role of protein phosphorylation in activation of phospholipase A_2 by the polychlorinated biphenyl mixture Aroclor 1242. Toxicol Appl Pharmacol 2000;163:9–16.
[73] McGahon B, Lynch MA. Analysis of the interaction between arachidonic acid and metabotropic glutamate receptor activation reveals that phospholipase C acts as a coincidence detector in the expression of long-term potentiation in the rat dentate gyrus. Hippocampus 1998;8:48–56.
[74] Adachi T, Nakashima S, Saji S, Nakamura T, Nozawa Y. Mitogen-activated protein kinase activation in hepatocyte growth factor-stimulated rat hepatocytes: involvement of protein tyrosine kinase and protein kinase C. Hepatology 1996;23:1244–53.
[75] Tudan C, Jackson JK, Pelech SL, Attardo G, Burt H. Selective inhibition of protein kinase C, mitogen-activated protein kinase, and neutrophil activation in response to calcium pyrophosphate dihydrate crystals, formyl-methionyl-leucyl-phenylalanine, and phorbol ester by *O*-(chloroacetyl-carbamoyl) fumagillol (AGM-1470; TNP-470). Biochem Pharmacol 1999;58:1869–80.
[76] Llansola M, Monfort P, Felipo V. Inhibitors of phospholipase C prevent glutamate neurotoxicity in primary cultures of cerebellar neurons. J Pharmacol Exp Ther 2000;292:870–6.
[77] Myhre O, Vestad TA, Sagstuen E, Aarnes H, Fonnum F. Effects of the solvent 1,2,4-trimethylcyclohexane on respiratory burst in human neutrophil granulocytes. A chemiluminescence and electron paramagnetic resonance spectrometry study. Ann N Y Acad Sci 1999;893: 358–61.
[78] Lin LL, Wartmann M, Lin AY, Knopf JL, Seth A, Davis RJ. $cPLA_2$ is phosphorylated and activated by MAP kinase. Cell 1993;72:269–78.
[79] Channon JY, Leslie CC. A calcium-dependent mechanism for associating a soluble arachidonoyl-hydrolyzing phospholipase A_2 with membrane in the macrophage cell line RAW 264.7. J Biol Chem 1990;265:5409–13.
[80] Ciani E, Groneng L, Voltattorni M, Rolseth V, Contestabile A, Paulsen RE. Inhibition of free radical production or free radical scavenging protects from the excitotoxic cell death mediated by glutamate in cultures of cerebellar granule neurons. Brain Res 1996; 728:1–6.